MDPI

Article

Theoretical study of the dissociative recombination and vibrational (de-)excitation of $HCNH^+$ and its isomers by electron impact

Mehdi Adrien Ayouz [1,*] and Arnaud Buch [2]

[1] LGPM, CentraleSupélec, Université Paris-Saclay, 8-10 rue Joliot-Curie, Gif-sur-Yvette, F-91190, France; mehdi.ayouz@centralesupelec.fr
[2] LGPM, CentraleSupélec, Université Paris-Saclay, 8-10 rue Joliot-Curie, Gif-sur-Yvette, F-91190, France; arnaud.buch@centralesupelec.fr
* Correspondence: mehdi.ayouz@centralesupelec.fr

Abstract: Protonated hydrogen cyanide, $HCNH^+$ is one of the most important molecule of interest in the astrophysical and astrochemical fields. In fact, this molecule not only plays the role of a reaction intermediary in various types of interstellar reaction, but was also identified in Titan's upper atmosphere. So, the cross sections for the dissociative recombination (DR) and vibrational (de-)excitation (VE and VDE) of $HCNH^+$ and its CNH_2^+ isomer are computed using a theoretical approach based on the combination of the normal modes approximation for the vibrational states of the target ions and the UK R-matrix code to evaluate electron–ion scattering matrices for fixed geometries of ions. The theoretical convoluted DR cross section for $HCNH^+$ agree well with the experimental data and a previous study. It is also found that the DR of the CNH_2^+ isomer is important which suggests that this ion might be present in DR experiments of $HCNH^+$. Moreover, the *ab initio* calculations performed on the H_2CN^+ isomer predict that this ion is a transition state. This result was confirmed by the study of reaction path of the $HCNH^+$ isomerization that was carried out by evaluating the intrinsic reaction coordinates (IRC). Finally, thermally averaged rate coefficients derived from the cross sections are provided for temperatures in the 10–10000 K range. A comprehensive set of calculations is performed to assess uncertainty of the obtained data. These results should help in modelling non-LTE spectra of $HCNH^+$, taking into account the role of its most stable isomer, in various astrophysical environments.

Keywords: molecular cation reactive collisions; dissociative recombination; vibrational excitation; R-matrix theory; interstellar medium; Titan's upper atmosphere; isomer

Citation: Ayouz, M. A.; Buch, A. Title. *Journal Not Specified* **2024**, *1*, 0. https://doi.org/

Received:
Revised:
Accepted:
Published:

1. Introduction

$HCNH^+$ is an important species in astrophysical environments such as dark interstellar molecular clouds (Sgr B2[1], TMC-1[2]), proto-star (L483[3]) or pre-stellar and mass starforming cores[4,5]. This molecule was also detected by the Ion and Neutral Mass Spectrometer (INMS) instrument aboard the Cassini probe in the upper atmosphere of Titan, Saturn's largest moon[6,7]. $HCNH^+$ could be an important precursor of the aerosols (Tholins) present on this satellite. The latter may themselves be the origin of molecules of prebiotic interest such as amino acids, nucleic acids, sugars or even more complex molecules such as proteins[8,9]. $HCNH^+$ is the simplest protonated nitrile, known as N-Protonated HCN or Protonated hydrogen cyanide. In the interstellar medium (ISM), it was often postulated that $HCNH^+$ is at the origin of the thermochemically unrealistic HNC/HCN abundance ratio [10]. HCN is one of the most interesting molecules for cosmochemistry, as it is considered by some to be one of the first molecules present on the prebiotic earth [11] and could, following polymerization and contact with water and oxygen, give rise to more complex molecules known to be the building blocks of life [12]. Observations in cold dark

clouds report values for the HNC/HCN isomer abundance ratio ranging from 0.015 to 5 [13,14] whereas theoretical study indicated that this abundance ratio should have an upper limit of one [15].

Due to the relatively large abundance of electrons and $HCNH^+$ in the ISM[10], collisions of $HCNH^+$ with electrons play a significant role, in particular, leading to dissociation (DR - dissociative recombination), vibrational (de-)excitation (VE, VDE) and rotational (de-)excitation of $HCNH^+$. The DR process leads to the formation of HCN or HNC while VE and VDE compete with the latter. Recent studies attempt to reproduce the observed $HCNH^+$ abundance, also responding to controversies over the HNC/HCN abundance ratio, within dense cold regions taking into account in their chemical models not only the DR process of $HCNH^+$[4] but also other formation paths for $HCNH^+$ (following $NH_3 + C^+$, for instance) [5], or destruction paths of HCN (in collision with oxygen, for example) [16], or excitation of $HCNH^+$ (in collision with H_2 and He, for example, accounting for the hyperfine structure of the target ion) [17]. In these studies, authors provided the updated $HCNH^+$ abundances in better agreement with the observations. Despite these enhancements, discrepancies between observations and predictions remain unresolved which requires a better understanding of the $HCNH^+$ chemistry in particular the DR process occurring in $HCNH^+$ and its isomers.

The DR mechanism of $HCNH^+$ was also subject to controversy. Indeed, Hickman *et al.* [18] supported that direct dissociative recombination process (when a doubly-excited state dissociating into neutral fragments crosses the ground state of the ion near its equilibrium geometry) could occur at low energy while Ngassan and Orel [19] found that the direct DR cross section is lower than the experimental value. Latter, Douguet *et al.* [20] demonstrated that the major contribution to the DR cross section at low electron collisional energies came out from indirect mechanism (electron captured into a vibrationally excited Rydberg state of the neutral molecule that couples to the doubly-excited state dissociating into neutral fragments). In that study, authors employed a theoretical approach based on the multichannel quantum defect theory (MQDT)[21,22]. After computing the *ab initio* potential energy surface (PES) of $HCNH^+$ and its series of Rydberg energies, the quantum defects are obtained from energies of excited Rydberg states. In the present study, we will employ instead of the quantum defect, the scattering matrix obtained from the UK molecular R-Matrix code (UKRMol) [23,24]. Thus, we revisited the DR cross section of $HNCH^+$ and compared it with the available experimental studies of Semaniak *et al.*[25], carried out at the heavy-ion storage ring CRYRING. As the authors of this study cannot exclude a possible involvement of other isomers, we also provided the first calculations for the CNH_2^+ isomer in its singlet state. This isomer was little studied, even by the scientific community interested in Titan. However, some authors such as Fortenberry *et al.* showed that this molecule could be present in a kinetically favorable potential well[26]. Moreover, *ab initio* calculations of the singlet ground state of the H_2CN^+ isomer was found with one imaginary frequency suggesting that the ion is unstable. This was confirmed by performing the $HCNH^+$ isomerization reaction path. Finally, the four lowest triplet states for isomers of $HCNH^+$ are not treated in the present study because these states are situated at very high energy, at least 5.3 eV above the singlet ground state of $HNCH^+$ [25,27].

The objective of this study is to demonstrate that the DR cross section of CNH_2^+ by electron impact is not negligible at low energy. Thus, this isomer could play an important role in the chemistry of $HCNH^+$, and must therefore be taken into account in chemical models that attempt to explain the thermochemically unrealistic HNC/HCN abundance ratio in the interstellar medium. The article is organized in the following way. After the above Introduction, Section 2 describes the theoretical approach used in the present calculations. The obtained cross sections and the corresponding rate coefficients are displayed and discussed in Section 3 while Section 4 concludes the study.

2. Theoretical approach

As the basic formalism employed in our model is presented in detail in Refs.[28–32], we only highlight in this section its major ideas.

2.1. The properties of $HCNH^+$ and its Isomers

2.1.1. $HCNH^+$ and its CNH_2^+ Isomer

$HCNH^+$ is a closed-shell molecule, having the symmetry of the $C_{\infty v}$ point group at equilibrium and ground state electronic configuration

$$X\,^1\Sigma : 1\sigma^2\,2\sigma^2\,3\sigma^2\,4\sigma^2\,5\sigma^2\,1\pi^4.$$

At low electron collisional energies, the ion can be characterized by five normal modes of vibration : three stretching modes ν_1, ν_2 and ν_3 with respective frequencies ω_1, ω_2 and ω_3 and corresponding coordinates q_1, q_2 and q_3, and two doubly degenerate transverse modes ν_4 and ν_5 with a lower frequencies ω_4 and ω_5, and coordinates $\left(q_{4x}, q_{4y}\right)$ and $\left(q_{5x}, q_{5y}\right)$. The normal coordinates and the related frequencies are obtained using the cc-pVTZ basis set centered on each atom and including s, p and d orbitals. Performing Coupled Cluster Singles, Doubles and Triples (CCSD(T)) calculations in the C_{2v} symmetry group, using the MOLPRO suite of codes [33], we found an equilibrium geometry of the ion for values of bond lengths (r_1, r_2, r_3) and bond angles $(\theta_1, \theta_2, \theta_3)$ given in Table 1. First columns of this table compare results obtained in the present calculation with theoretical data while the upper panel of Figure 1 shows normal displacements for each mode of $HCNH^+$ with the bond lengths and bond angles of Table 1 depicted for the first normal mode.

Table 1. Bond lengths (r_1, r_2 and r_3 in Å) and bond angles (θ_1, θ_2 and θ_3 in degree) at the equilibrium geometry of $HCNH^+$ and its CNH_2^+ isomer, both displayed in Figure 1. The total energies are given in atomic units. Data obtained in this study are compared to the calculations of Ref.[34].

	$HCNH^+$		CNH_2^+	
Geometry	**This study**	**Calc.**	**This study**	**Calc.**
r_1	1.0803	1.0804	1.2514	1.2514
r_2	1.1403	1.1403	1.0326	1.0327
r_3	1.0139	1.0140	1.0326	1.0327
θ_1	180	180	120.979	120.988
θ_2	180	180	120.979	120.988
θ_3	0	0	118.041	118.024
Total energy	-93.557075	-93.557076	-93.475788	-93.475788

N-protonated hydrogen isocyanide CNH_2^+ is one of the isomer of $HCNH^+$ belonging to the C_{2v} point group at equilibrium geometry. Its ground state electronic configurations is

$$1\,^1\mathrm{A}_1 : 1a_1^2\,2a_1^2\,3a_1^2\,4a_1^2\,1b_2^2\,1b_1^2\,5a_1^2.$$

This isomer has six non-degenerate normal modes ν_i with respective frequencies ω_i and corresponding coordinates q_i $(i = 1, 2, 3, 4, 5, 6)$. Analogously, the normal coordinates and the related frequencies are obtained using the CCSD(T) method and cc-pVTZ basis set. Table 1 gives the obtained calculations. Bond lengths and bond angles are given in Table 1 and normal displacements for each mode are shown in Figure 1. The calculations agree pretty well with data available in the literature.

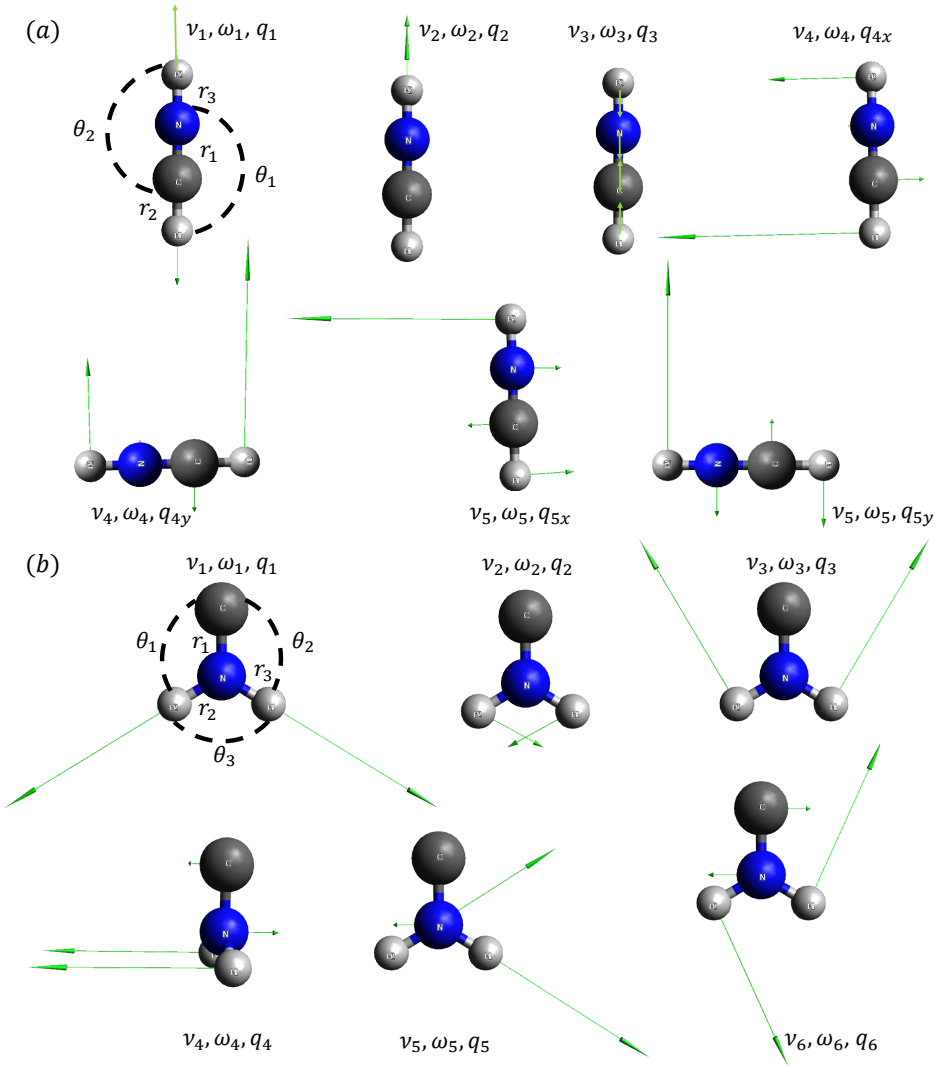

Figure 1. Normal modes of (**a**) $HCNH^+$ with (**b**) its CNH_2^+ isomer. Bond lengths and bond angles of each ion (listed in Table 2) are depicted on the first normal mode sketch of each panel. The arrows indicate the direction and magnitude of displacements for each mode. Note that arrowheads are not shown for the displacements of relatively large magnitudes.

Table 2. Vibrational frequencies (ω_i in cm^{-1}) obtained in this study for $HCNH^+$ and its CNH_2^+ isomer are compared with previous data available in literature (experimental or theoretical data).

$HCNH^+$

Normal mode, ν_i	Symmetry	Normal coordinate, q_i	Frequency, ω_i	
			This study	Exp.[34]
NH stretch, ν_1	Σ	q_1	3645.07	3482.8
CH stretch, ν_2	Σ	q_2	3316.36	3187.9
CN stretch, ν_3	Σ	q_3	2179.51	2155.7
HCN bend, ν_4	Π	q_{4x}, q_{4y}	805.33	801.6
HNC bend, ν_5	Π	q_{5x}, q_{5y}	647.86	645.9

CNH_2^+

Normal mode, ν_i	Symmetry	Normal coordinate, q_i	Frequency, ω_i	
			This study	Calc.[34]
ν_1	A_1	q_1	3317	3318
ν_2	A_1	q_2	1723	1724
ν_3	A_1	q_3	1394	1394
ν_4	B_1	q_4	723	725
ν_5	B_2	q_5	3405	3405
ν_6	B_2	q_6	630	627

2.1.2. The H_2CN^+ Isomer

In the literature [27,35,36], it was reported the existence of another singlet state of the $HCNH^+$ isomer with hydrogen atoms next to carbon, also known as hydrocyanonium cation H_2CN^+ which belongs to the C_{2v} point group at equilibrium geometry. Its ground state electronic configuration is

$$^1A_1 : 1a_1^2\, 2a_1^2\, 3a_1^2\, 4a_1^2\, 1b_2^2\, 5a_1^2\, 1b_1^2\,,$$

with a total energy of -93.440025 (atomic units). This isomer have also six non-degenerate normal modes ν_i with respective frequencies ω_i and corresponding coordinates q_i $(i = 1, 2, 3, 4, 5, 6)$. Performing the Molpro calculations, the normal coordinates and the related frequencies was obtained using the CCSD(T) method and cc-pVTZ basis set. Table 3 compares the results with data available in the literature [34]. As expected, we found that the H_2CN^+ isomer has the normal mode ν_6 with imaginary frequency ω_6 corresponding to the torsional movement of the H atoms and to the N-H stretch. This result suggests that the isomer is unstable with respect to isomerization into the $HCNH^+$ linear form.

To verify the nature of the eventual transition state obtained, we determined the reaction path throughout the intrinsic reaction coordinates (IRC) by invoking the Quadratic Steepest Descent Reaction Path method (QSDPATH) implemented in MOLPRO[33]. The IRC is defined similarly to the minimum energy path (MEP) but instead of the steepest-descent path on the potential energy surface, IRC follows the maximum instantaneous acceleration from the transition state (TS) down towards a local minimum. IRC is in fact the solution of a differential equation of the mass-weighted Cartesian coordinates with respect to the coordinate along the IRC. See for example Ref.[37] for more details.

Starting from the equilibrium geometry of H_2CN^+, obtained after optimisation (see Table 3), we performed IRC calculations and found that the linear structure $HCNH^+$ is predicted to lie lower by 3.18 eV. The lower panel of Figure 2 shows the total energy (in atomic units) and the upper panel the bond lengths and angles along the IRC (in atomic units). Following the positive direction in reaction path (blue arrow in the lower panel of the figure), the migration of a hydrogen atom (here H1) from carbon to nitrogen led to the formation of the more stable linear isomer $HCNH^+$ with bond lengths and angles characteristics given in Table 1. Analogously, the migration of the second hydrogen atom (H2) to nitrogen, in case of negative IRC direction (violet arrow in the lower panel of the figure), gives the same molecular ion configuration. The sketch in the lower panel of that

figure displays both migration processes with a color code according to the bond length and angles curves. Thus, the reaction path of the $HCNH^+$ isomerization confirms that the H_2CN^+ isomer is a transition state which could explain why it has not yet been identified in interstellar space.

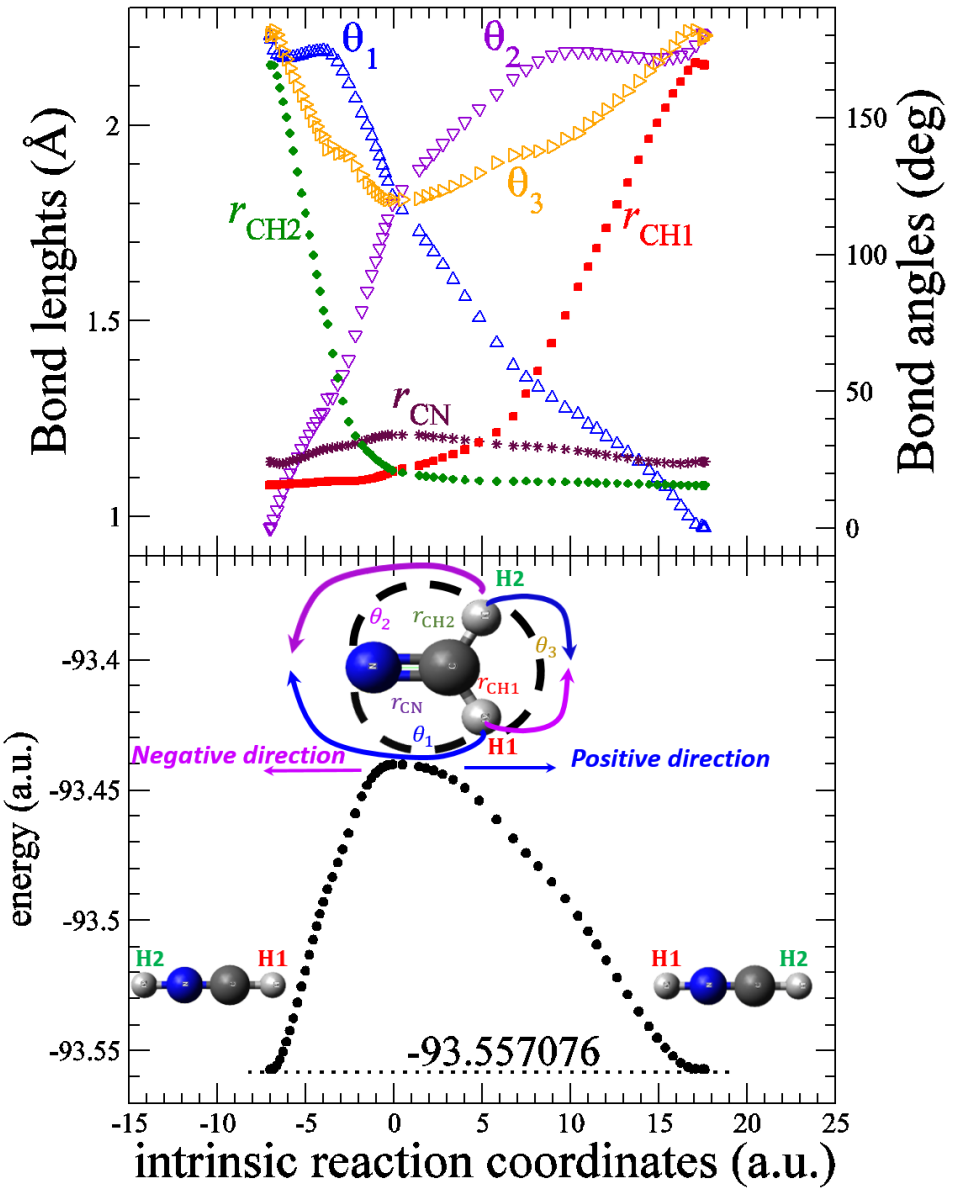

Figure 2. Reaction path of the $HCNH^+$ isomerization. The upper panel of the figure shows the dependence of bond lengths (maroon-r_{CN}, red-r_{CH1} and green-r_{CH2}) and bond angles (blue-θ_1, violet-θ_2 and orange-θ_3) as functions of IRC. Bond lengths are given in circle, square and star symbols with values on the left axis, while the bond angles are given with triangle symbols with values on the right axis. In the lower panel, a sketch of the migration process of hydrogen atoms from carbon to nitrogen is depicted according to the same color code. The total energy is displayed in black circles. Whatever the direction in the IRC, positive in blue arrows or negative in violet arrows, the migration process leads to the most stable linear isomer $HCNH^+$ (see Table 1).

2.2. Fixed-geometry Scattering Matrix

In our model, the fixed-nuclei reactance matrix (K-matrix) is employed to describe the e-$HCNH^+$ isomers collisions. It is obtained numerically for each geometry configuration

Table 3. Vibrational frequencies (ω_i in cm^{-1}) obtained in this study for the H_2CN^+ isomer are compared with previous calculations available in literature. Note that the normal mode ν_6 has an imaginary frequency ω_6. Table below gives Bond lengths (in Å) and bond angles (in degree). A sketch of the employed coordinates is given in the lower panel of Figure 2

Mode, ν_i	**Symmetry**	**Normal coordinate,** q_i	**Frequency,** ω_i	
			This study	**Calc.[34]**
ν_1	A_1	q_1	2862	2859
ν_2	A_1	q_2	1843	1843
ν_3	A_1	q_3	1034	1025
ν_4	B_1	q_4	810	804
ν_5	B_2	q_5	2897	2892
ν_6	B_2	q_6	$\imath$437	$\imath$456

Geometry	**This study**	**Calc.[34]**
r_{CN}	1.2089	1.2089
r_{CH1}	1.1169	1.1168
r_{CH2}	1.1169	1.1168
θ_1	119.950	119.927
θ_2	119.950	119.927
θ_3	120.099	120.145

of the target molecule using the UK molecular R-Matrix code (UKRMol) [23,24] with the Quantemol-N expert system [38].

R-matrix calculations are performed in the C_1 point group for a given ion in its ground electronic state. The four $1a^2\,2a^2$ core electrons are frozen and ten electrons are kept distributed in the active space including $3-11a$ molecular orbitals. For each ion, a total number of 5292 configuration state functions (CSFs) are used for the ground state. All the generated states up to 10 eV were retained in the final close-coupling calculation. We employed an R-matrix sphere of radius 12 bohrs and a partial-wave expansion with continuum Gaussian-type orbitals up to $l \leq 4$. In the following, this calculation with the cc-pVTZ basis set and the complete active space (CAS_1) described above will be referred to Model 1.

K-matrices are obtained from the R-matrix calculations for a geometry configuration of the ion specified by the normal coordinates $\mathbf{q} = \{q_1, q_2, \ldots, q_n\}$ with n being the number of normal modes. $K(\mathbf{q})$ is transformed into scattering matrix as $S(\mathbf{q}) = (1 + \imath K(\mathbf{q}))(1 - K(\mathbf{q}))^{-1}$. At low collisional energies $S(\mathbf{q})$ depends only weakly on energy while a sharper energy dependence is observed at certain relatively high energies, corresponding to positions of Rydberg states attached to the excited electronic states of the ion. The eigenphase sum is a convenient way to identify a weak or a strong energy dependence of the scattering matrix. Figure 3 shows eigenphase sum for the equilibrium geometry ($q_0 = 0.01$) and displacement $q_i = 0.1$ along each normal mode ν_i of both ions. The variation of the eigenphase sums is smooth for energies below 1 eV and 0.3 eV for $HCNH^+$ and CNH_2^+, respectively. Above these values, a sharp energy dependence at certain energies (at 3.4 eV for $HCNH^+$ and 0.46 eV for CNH_2^+, for instance) is observed due to the presence of electronic Rydberg resonances attached to closed ionization limits.

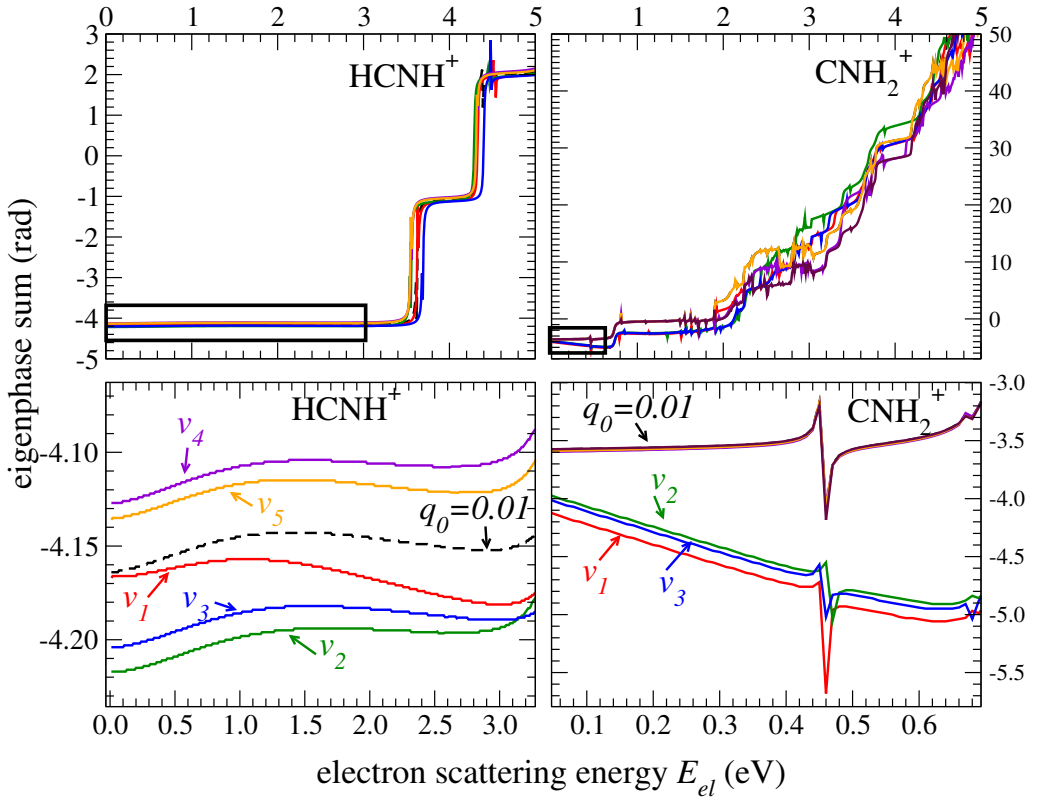

Figure 3. Eigenphase sum as a function of the electron scattering energy E_{el} for equilibrium geometry $q_0 = 0.01$ and displacements $q_i = 0.1$ along each normal mode ν_i of $HCNH^+$ (left panels) and CNH_2^+ (right panels). The lower panels show for each ion an enlarged view at low collisonnal energies corresponding to the black thick rectangles. The curves are color coded according the normal mode labels ν_i. The equilibrium geometry is depicted in black dashed curves for both ions. Note that the curves of the equilibrium geometry and normal modes $\nu_{3,4,5}$ of CNH_2^+ isomer are indistinguishable.

2.3. Formulas of the dissociative recombination and vibrational (de-)excitation cross sections

The following assumptions are employed in the present model : (i) the rotation of the molecular ions is neglected, (ii) the cross-section is averaged over the autoionizing resonances, (iii) the autoionization lifetime is assumed to be much longer than the predissociation lifetime and (iv) the harmonic approximation is used to describe the vibrational state of the core ion. For more details see Ref.[28].

Combining the above assumptions (i)–(iv) and applying the frame transformation, the vibrational excitation (VE) and de-excitation (VDE) cross-sections are given, in terms of expanded scattering matrix elements to the first order of the normal coordinates, as follows :

$$\sigma_i^{VE}(E_{el}) = \frac{\pi\hbar^2}{2mE_{el}} P_i \theta(E_{el} - \hbar\omega_i) \tag{1}$$

and

$$\sigma_i^{VDE}(E_{el}) = \frac{\pi\hbar^2}{2mE_{el}} P_i \,, \tag{2}$$

where

$$P_i \quad = \tfrac{g_i}{2} \sum_{ll'\lambda\lambda'} \left| \frac{\partial S_{l\lambda l'\lambda'}}{\partial q_i} \right|^2_{q_0} \tag{3}$$

is a quantity that can be interpreted as the probability of excitation of the vibrational mode ν_i. Above, q_i, $\hbar\omega_i$ and g_i $(i = 1 - n)$ are respectively the dimensionless coordinate, the energy and the degeneracy of the mode ν_i with n stands for the number of normal coordinates. Again q_0 is the equilibrium geometry of the target ion. For the linear molecular ion $HCNH^+$, $n = 5$ with a degeneracy of $g_4 = 2$ and $g_5 = 2$ for bending modes 4 and 5 and $g_{1-3} = 1$ for the stretching modes 1, 2 and 3. In case of the CNH_2^+ isomer, $n = 6$ with a degeneracy of $g_{1-6} = 1$ (see Table 2).

In the previous equations, $S_{l\lambda,l'\lambda'}$ is an element of the fixed-nuclei scattering matrix for electron-ion collisions with the initial channel (λl) and the exit channel $(\lambda' l')$, l being the electron angular momentum and λ its projections on the molecular axis. Finally, m is the reduced mass of the electron-ion system and E_{el} the incident energy of the electron. θ in Eq.(1) stands for the Heaviside step function.

In the present theoretical approach, the initial state of a given ion is its ground vibrational level, so the electron can only be captured into the first excited vibrational state of each normal mode of the ion. Formulas of Eqs.(1) and (2) give the VE and VDE cross sections for changing one quantum in each normal mode. Based on the propensity rule, (de-)excitation process changing two or more quanta is neglected in this study because their contributions in the cross sections are small.

As for the dissociative recombination (DR) process, the cross section is obtained [28] as

$$\left\langle \sigma^{DR}(E_{el}) \right\rangle = \frac{\pi\hbar^2}{2mE_{el}} \sum_{i=1}^{n} P_i \theta(\hbar\omega_i - E_{el}) \,, \tag{4}$$

where the bracket stands for the temporary captures in all the accessible Rydberg states. The present model suggests that the electron scattering energy is not sufficient to excite the ion and then to leave it. The probability of excitation P_i of the ion by the electron is described by the same physics : The electron is captured in a Rydberg resonance attached to the vibrational state excited by the electron. In such situation, the system electron-ion will most likely dissociate (DR process), rather then autoionize (VE process of Eq.(1)).

Finally, to calculate the excitation probabilities P_i, the derivative of the scattering matrix with respect to the normal coordinate q_i, the scattering matrix is evaluated for two values of q_i, $q_i = 0.01$ and $q_i = 0.1$, keeping the other normal coordinates fixed at the equilibrium geometry, i.e. $q_0 = 0.01$.

3. Results and discussions

3.1. Cross Sections

In the theoretical model described above, we assumed that the excitation probabilities are energy-independent. Figure 4 shows the weak dependence of P_i of Eq.(3) on energy. As demonstrated in Figure 3 for the eigenphase sums, those quantities are constants at low energies, and therefore could be used in the calculations of cross sections of Eq. (1), (2) and (4) as well as for thermally averaged rate coefficients, given in the next section.

Table 5 presents the largest vibronic interactions in both molecules and along each normal coordinate. The couplings are given in the form of partial derivative, with respect to the normal coordinates, of the scattering matrix. Several observations can be made from the values and form of the couplings. It is appears that the indirect DR cross section of $HCNH^+$ will be larger than that of the isomer. As excepted for linear polyatomic ions, the vibronic interactions mediated by the molecular bending is responsible for the indirect DR mechanism in $HCNH^+$. However, the present results show also that the contribution from the vibronic interactions induced by stretching modes of the ion is also important, as reported in Ref.[28] for HCO^+ and N_2H^+. Furthermore, the most interesting point is certainly the unexpected high values of the vibronic couplings in the CNH_2^+ isomer. This result implies a large cross section for that ion.

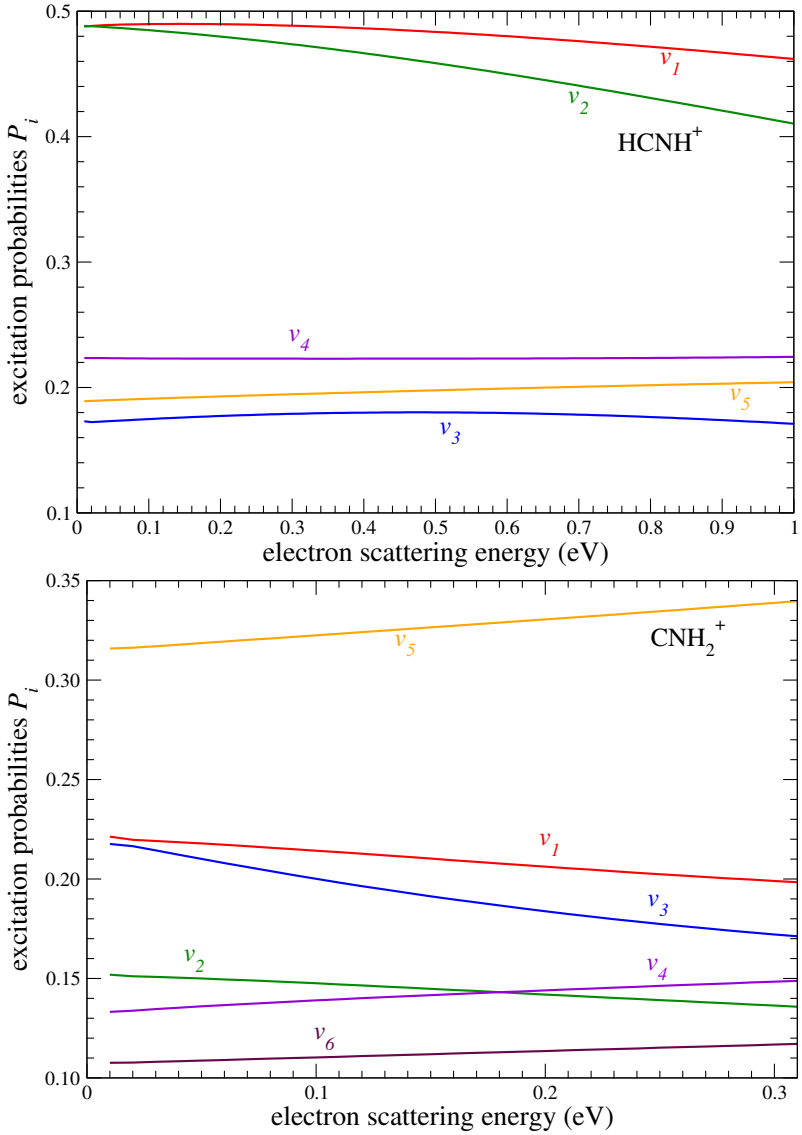

Figure 4. VE probabilities of Eq.(3) corresponding to the normal vibrational modes of $HCNH^+$ (the upper panel) and CNH_2^+ (the lower panel). The color scheme corresponds to Figure 3.

Table 4. Parameters of equations (1), (2), (3) and (4) calculated at $E_{el} = 0.01$ eV collision energy.

Normal mode, ν_i	**HCNH$^+$** P_i	**CNH$_2^+$** P_i
1	0.4877205	0.2213105
2	0.4882937	0.1519490
3	0.1729784	0.2175728
4	0,4469524	0.1332123
5	0,3781402	0.3158785
6	-	0.1075744

Table 5. Partial derivatives with respect to the normal coordinates of the largest scattering matrix element for $HCNH^+$ and CNH_2^+ molecular ions at $E_{el} = 0.01$ eV.

	$HCNH^+$		**CNH_2^+**	
Normal mode, ν_i	**Electronic states** $l\lambda - l'\lambda'$	$\left\vert\frac{\partial S_{l\lambda l'\lambda'}}{\partial q_i}\right\vert_{q_0}$	**Electronic states** $l\lambda - l'\lambda'$	$\left\vert\frac{\partial S_{l\lambda l'\lambda'}}{\partial q_i}\right\vert_{q_0}$
1	$p\sigma - d\sigma$	0.4598	$s\sigma - s\sigma$	0.2345
2	$p\sigma - d\sigma$	0.4793	$d\delta - d\delta$	0.2149
3	$p\sigma - p\sigma$	0.3446	$d\delta - d\delta$	0.2963
4	$d\pi - d\pi$	0.3392	$d\delta - p\pi$	0.2308
5	$d\pi - d\pi$	0.2206	$p\pi - d\delta$	0.3322
6	-	-	$p\pi - p\sigma$	0.1672

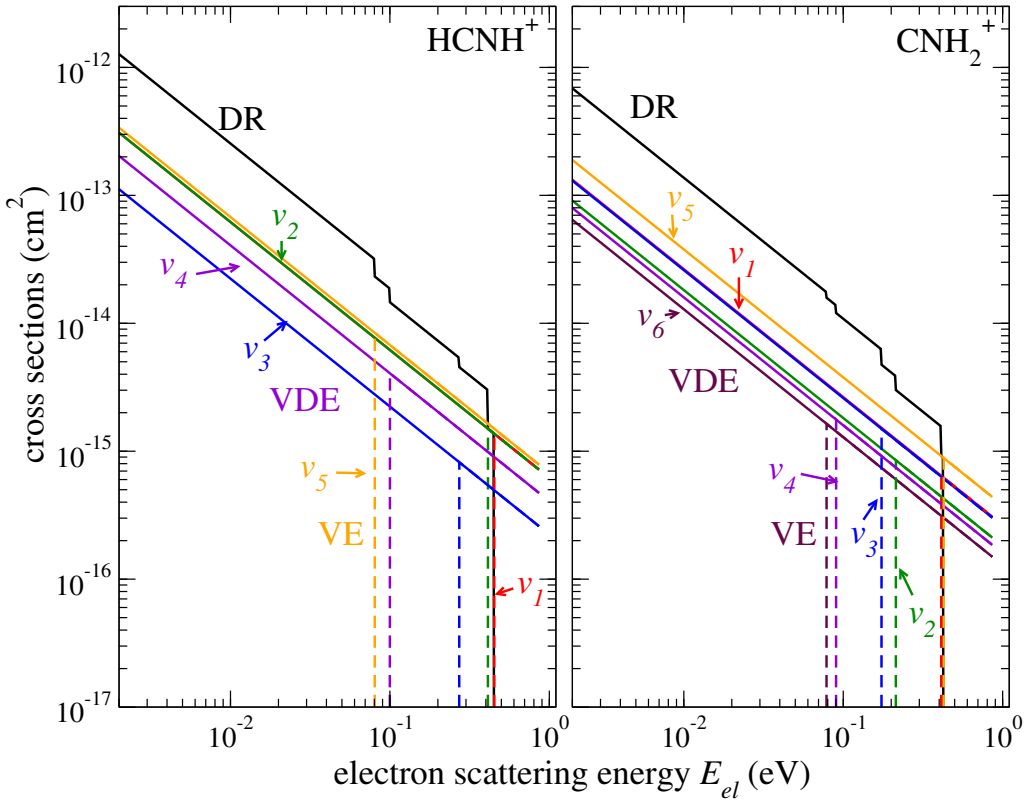

Figure 5. Theoretical VE, VDE and DR cross sections of $HCNH^+$ (left panel) and CNH_2^+ (right panel). Values of Table 4 was employed for this plot. The color scheme corresponds to Figure 4.

The theoretical VE, VDE and DR cross sections are displayed in Figure 5 for $HCNH^+$ (left panel) and CNH_2^+ (right panel). At low energies VE and DR cross sections are featureless and behave simply as $1/E_{el}$ following the Wigner law. For energies higher than 0.1 eV, the cross section drops in a stepwise manner because the scattering electron excites the vibrational level of the ion by one quanta.

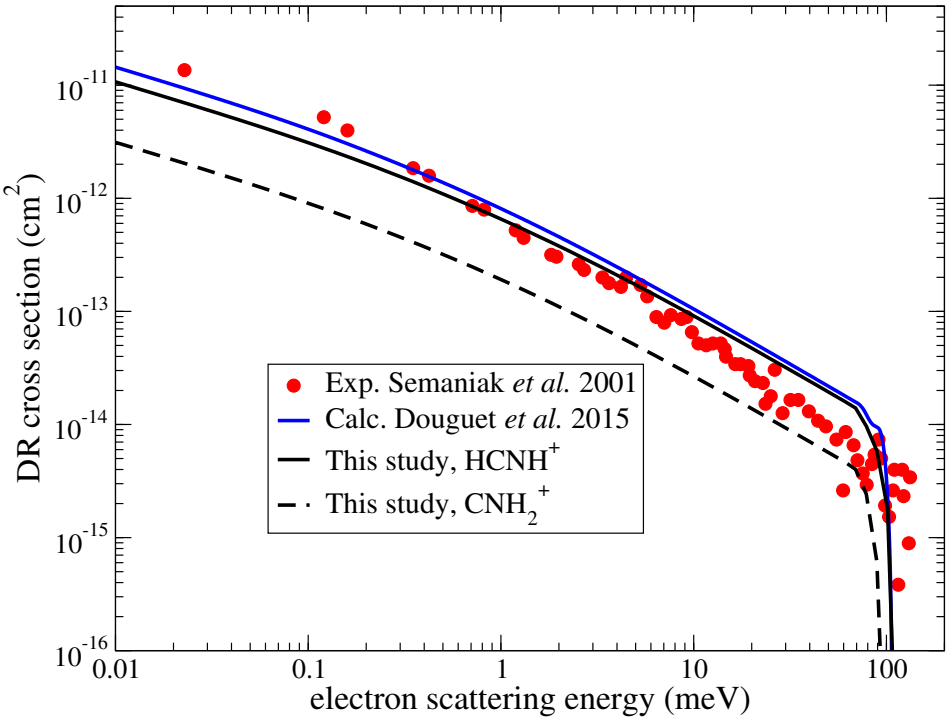

Figure 6. Theoretical DR cross section of $HCNH^+$ (solid black curve) obtained in this study compared to the experimental data (red dots) from Ref.[25] and previous theoretical result (solid blue curve) of Ref.[20]. DR cross section of CNH_2^+ (dashed black curve) obtained in this work is also displayed.

Figure 6 shows the theoretical cross section in comparison with the experimental results by Semaniak *et al.* [25] and previous calculations by Douguet *et al.* [20]. The cross section was convoluted according to Eq. (2) of Ref.[39] with a parallel electron energy of 0.1 meV and a transverse energy spread of 2 meV. One interesting feature for $HCNH^+$ is the double drop in its theoretical DR cross section corresponding to the two transverse normal modes ν_4 and ν_5, with very different asymmetrical elongations of the hydrogen atoms (see Table 2). There is a good agreement between the present result and previous theoretical and experimental data. The figure demonstrates that the DR cross section in CNH_2^+ isomer is also important presenting a drop at about 90 meV, which corresponds to the vibrational thresholds of ν_4 and ν_6 normal modes.

3.2. Rate Coefficients

Thermally averaged rate coefficients are evaluated from the general expression of Maxwell-Boltzmann averaging (see Eq.(7) of Ref.[40], for instance). Due to the simple analytical forms of the cross sections (1), (2) and (4), thermally averaged rate coefficients take the the following expressions

$$\alpha_i^{VE}(T) = \sqrt{\frac{2\pi}{k_b T}}\frac{\hbar^2}{m^{3/2}}\, P_i\, \exp\left(-\frac{\hbar\omega_i}{k_b T}\right), \tag{5}$$

$$\alpha_i^{VDE}(T) = \sqrt{\frac{2\pi}{k_b T}}\frac{\hbar^2}{m^{3/2}}\, P_i, \tag{6}$$

$$\alpha^{DR}(T) = \sqrt{\frac{2\pi}{k_b T}}\frac{\hbar^2}{m^{3/2}}\, \sum_{i=1}^{n} P_i \left[1-\exp\left(-\frac{\hbar\omega_i}{k_b T}\right)\right], \tag{7}$$

where k_b is the Boltzmann coefficient, m is the electron mass and T is the temperature. Figure 7 shows the obtained rate coefficients for VE, VDE and DR as functions of temperature. For low temperatures, $T < 500$ K, the VDE and DR rate coefficients behave as $1/\sqrt{T}$ while

for the VE $T^{-0.5}\exp\left(-\frac{\hbar\omega_i}{k_b T}\right)$. At higher temperatures, the DR rate coefficient decreases faster than $1/\sqrt{T}$ because the vibrational excitation becomes more probable.

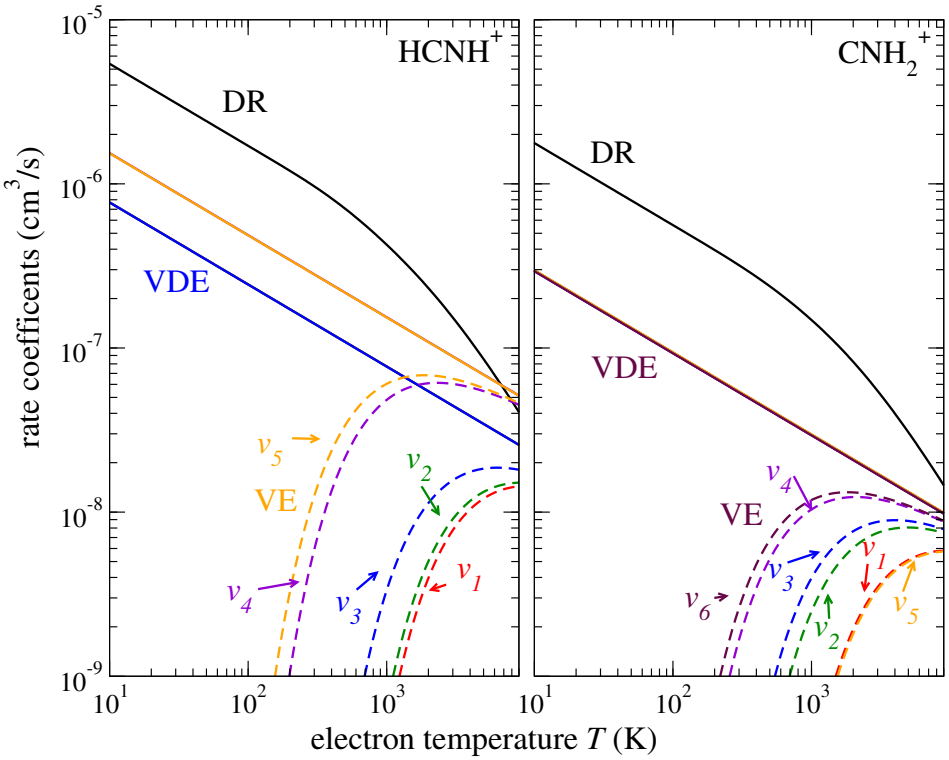

Figure 7. Theoretical VE, VDE and DR rate coefficents of $HCNH^+$ (left panel) and CNH_2^+ (right panel). Values of Table 4 was employed for this plot. The color scheme corresponds to Figure 6.

3.3. Assessment of Uncertainties

The main identifiable sources of uncertainty is the scattering model used in the calculation. To assess the associated uncertainty, we performed a complete calculation of the VE, VDE and DR cross sections using different basis sets and orbital spaces in the electron-scattering calculations. The main scattering model (Model 1) is described in Section 2.2. In the second set of calculations (Model 2), the electronic basis was reduced from cc-pVTZ to DZP. In Model 3, the complete active space (CAS) in the configuration interaction calculations was reduced with respect to Model 1 by 2 orbitals, i.e. 3*a* and 4*a*.

Figure 8 shows the obtained results. The difference between the DR cross section produced in the three calculations is about 10% for $HCNH^+$ and 15% for the CNH_2^+ isomer. This later result implies that the DR cross section of CNH_2^+ is also important which suggests that this ion might be present in DR experiments of $HCNH^+$[25].

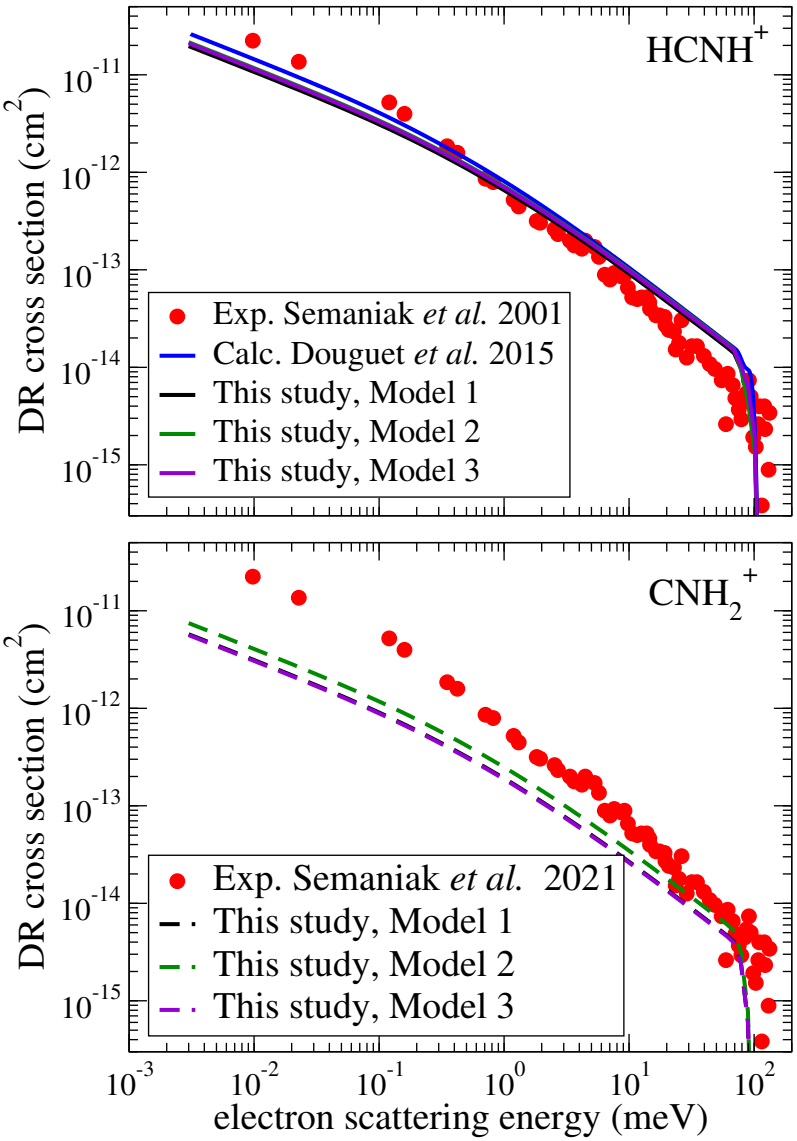

Figure 8. DR cross section obtained within three different scattering models (see text) in comparison with experiment and previous calculations (see Figure 6). Upper panel shows the obtained results for $HCNH^+$ (solid colored lines) while the lower panel for CNH_2^+ (dashed colored lines). The Model 1 is described in Section 2.2. In the Model 2, the basis to represent the electronic wave functions is reduced. In the Model 3, the orbital space in the configuration interaction calculation was reduced with respect to that used in the Model 1. The differences between results obtained in the three models are about 10% for $HCNH^+$ and 15% CNH_2^+, so that they are indistinguishable in the figure.

4. Conclusions

To summarize the results of the present study. We computed cross sections and rate coefficients for VE, VDE and DR of $HCNH^+(X\,^1\Sigma)$ and its stable isomer $CNH_2^+(1\,^1A_1)$ by electron impact using a theoretical approach that combines the normal modes approximation for the vibrational states of the target ions, the vibrational frame transformation, and the UK R-matrix code.

The convoluted DR cross section for $HCNH^+$ agrees pretty well with the experimental data and a previous study. Another interesting feature is the importance of the DR cross section of CNH_2^+ isomer which suggests that this ion could be present in the DR experiment of $HNCH^+$. To confirm these findings, a comprehensive set of calculations was performed to assess uncertainty of the obtained cross sections.

Since the cross sections and thermally averaged rate coefficients have a simple analytical forms, they can readily used in the modeling of non-LTE spectra of $HCNH^+$, involving the CNH_2^+ isomer, in various astrophysical environments. These results demonstrate that CNH_2^+ must to be taken into account in chemical models that attempt to explain the $HCNH^+$ abundance and HNC/HCC abundance ratio observed in the interstellar medium.

Moreover, the *ab inito* calculations preformed on the lowest singlet state of the H_2CN^+ isomer provided an imaginary frequency for one of its normal mode which suggests that the ion is likely unstable. A study of the $HCNH^+$ isomerization reaction path was performed by determining the intrinsic reaction coordinates (IRC). The linear structure $HCNH^+$ was found to lie lower by 3.18 eV. This proves that the H_2CN^+ isomer is a transition state explaining probably why it has not yet been identified in interstellar space.

Finally, the rotational structure of the target ions and of the neutral molecules was neglected in the present approach. Hence, the obtained cross sections and rate coefficients should be viewed as averaged over initial rotational states and summed over final rotational states corresponding to the initial and final vibrational levels (for VE and VDE) or dissociative states (for DR). Discrepancies between the computed results and the experimental measurements observed at low electron scattering energy maybe due to neglecting the rotational structure in the present model. Rotationally resolved cross sections, i.e. without changing the vibrational state will be the subject of a further study.

Author Contributions: Authors contributed equally to this work.

Funding: This research was funded by the Transatlantic Mobility Program of the Office for Science and Technology of the Embassy of France in the United States, Programme National "Physique et Chimie du Milieu Interstellaire" (PCMI) of CNRS/INSU and by the program "Accueil des chercheurs étrangers" of CentraleSupélec.

Acknowledgments: We acknowledge Viatcheslav Kokoouline for informative discussions and providing the DR theoretical and experimental data.

Conflicts of Interest: The authors declare no conflicts of interest.

References

1. Ziurys, L.M.; Turner, B.E. $HCNH^+$: A New Interstellar Molecular Ion. **1986**, *302*, L31. https://doi.org/10.1086/184631.
2. Schilke, P.; Walmsley, C.M.; Millar, T.J.; Henkel, C. Protonated HCN in molecular clouds. **1991**, *247*, 487.
3. Agúndez, M.; Cabezas, C.; Marcelino, N.; Fuentetaja, R.; Tercero, B.; de Vicente, P.; Cernicharo, J. A new protonated molecule discovered in TMC-1: $HCCNCH^+$. **2022**, *659*, L9, [arXiv:astro-ph.GA/2203.06999]. https://doi.org/10.1051/0004-6361/202243396.
4. Quénard, D.; Vastel, C.; Ceccarelli, C.; Hily-Blant, P.; Lefloch, B.; Bachiller, R. Detection of the HC_3NH^+ and $HCNH^+$ ions in the L1544 pre-stellar core. *Monthly Notices of the Royal Astronomical Society* **2017**, *470*, 3194–3205, [https://academic.oup.com/mnras/article-pdf/470/3/3194/18548190/stx1373.pdf]. https://doi.org/10.1093/mnras/stx1373.
5. Fontani, F.; Colzi, L.; Redaelli, E.; Sipilä, O.; Caselli, P. First survey of $HCNH^+$ in high-mass star-forming cloud cores. **2021**, *651*, A94, [arXiv:astro-ph.GA/2105.08732]. https://doi.org/10.1051/0004-6361/202140655.
6. Cravens, T.E.; Robertson, I.P.; Waite Jr., J.H.; Yelle, R.V.; Kasprzak, W.T.; Keller, C.N.; Ledvina, S.A.; Niemann, H.B.; Luhmann, J.G.; McNutt, R.L.; et al. Composition of Titan's ionosphere. *Geophysical Research Letters* **2006**, *33*, [https://agupubs.onlinelibrary.wiley.com/doi/pdf/10.1029/2005GL025 https://doi.org/doi.org/10.1029/2005GL025575.
7. Vuitton, V.; Yelle, R.; McEwan, M. Ion chemistry and N-containing molecules in Titan's upper atmosphere. *Icarus* **2007**, *191*, 722–742. https://doi.org/https://doi.org/10.1016/j.icarus.2007.06.023.
8. d'Ischia, M.; Manini, P.; Moracci, M.; Saladino, R.; Ball, V.; Thissen, H.; Evans, R.A.; Puzzarini, C.; Barone, V. Astrochemistry and Astrobiology: Materials Science in Wonderland? *International Journal of Molecular Sciences* **2019**, *20*. https://doi.org/10.3390/ijms20174079.

9. Kawai, J.; Kebukawa, Y.; McKay, C.P.; Kobayashi, K. Nucleic acid bases in Titan tholins and possible genetic systems in the Titan liquidosphere. *Life Sciences in Space Research* **2019**, *20*, 20–29. https://doi.org/https://doi.org/10.1016/j.lssr.2018.11.002.
10. Watson, W.D. Ion-Molecule Reactions, Molecule Formation, and Hydrogen-Isotope Exchange in Dense Interstellar Clouds. **1974**, *188*, 35–42. https://doi.org/10.1086/152681.
11. Ferris, J.P.; Hagan, W.J. HCN and chemical evolution: The possible role of cyano compounds in prebiotic synthesis. *Tetrahedron* **1984**, *40*, 1093–1120. https://doi.org/https://doi.org/10.1016/S0040-4020(01)99315-9.
12. Matthews, C.N.; Minard, R.D. Hydrogen cyanide polymers, comets and the origin of life. *Faraday Discuss.* **2006**, *133*, 393–401. https://doi.org/10.1039/B516791D.
13. Goldsmith, P.F.; Langer, W.D.; Ellder, J.; Kollberg, E.; Irvine, W. Determination of the HNC to HCN abundance ratio in giant molecular clouds. **1981**, *249*, 524–531. https://doi.org/10.1086/159312.
14. Irvine, W.M.; Schloerb, F.P. Cyanide and isocyanide abundances in the cold, dark cloud TMC-1. **1984**, *282*, 516–521. https://doi.org/10.1086/162229.
15. Sarrasin, E.; Abdallah, D.B.; Wernli, M.; Faure, A.; Cernicharo, J.; Lique, F. The rotational excitation of HCN and HNC by He: new insights on the HCN/HNC abundance ratio in molecular clouds. *Monthly Notices of the Royal Astronomical Society* **2010**, *404*, 518–526, [https://academic.oup.com/mnras/article-pdf/404/1/518/11182515/mnras0404-0518.pdf]. https://doi.org/10.1111/j.1365-2966.2010.16312.x.
16. Gong, Y.; Du, F.J.; Henkel, C.; Jacob, A.M.; Belloche, A.; Wang, J.Z.; Menten, K.M.; Yang, W.; Quan, D.H.; Bop, C.T.; et al. Protonated hydrogen cyanide as a tracer of pristine molecular gas. **2023**, *679*, A39, [arXiv:astro-ph.GA/2308.15521]. https://doi.org/10.1051/0004-6361/202347409.
17. Bop, Cheikh T..; Agùndez, Marcelino.; Cernicharo, Jose.; Lefloch, Bertrand.; Lique, Franoiçs. $HCNH^+$ abundance in cold dense clouds based on the first hyperfine resolved rate coefficients. *AA* **2024**, *681*, L19. https://doi.org/10.1051/0004-6361/202348947.
18. Hickman, A.P.; Kashinski, D.O.; Malenda, R.F.; Gatti, F.; Talbi, D. Calculation of dissociating autoionizing states using the block diagonalization method: Application to N2H. *Journal of Physics: Conference Series* **2011**, *300*, 012016. https://doi.org/10.1088/1742-6596/300/1/012016.
19. Ngassam, V.; Orel, A.E. Resonances in low-energy electron scattering from $HCNH^+$. *Phys. Rev. A* **2007**, *75*, 062702. https://doi.org/10.1103/PhysRevA.75.062702.
20. Douguet, N..; Santos, S. Fonseca dos.; Kokoouline, V..; Orel, A.E.. Simplified model to describe the dissociative recombination of linear polyatomic ions of astrophysical interest. *EPJ Web of Conferences* **2015**, *84*, 07003. https://doi.org/10.1051/epjconf/20158407003.
21. Seaton, M. Quantum defect theory I. General formulation. *Proceedings of the Physical Society* **1966**, *88*, 801.
22. Greene, C.H.; Jungen, C. Molecular applications of quantum defect theory. In *Advances in atomic and molecular physics*; Elsevier, 1985; Vol. 21, pp. 51–121.
23. Tennyson, J. Electron–molecule collision calculations using the R-matrix method. *Phys. Rep.* **2010**, *491*, 29–76.
24. Carr, J.; Galiatsatos, P.; Gorfinkiel, J.; Harvey, A.; Lysaght, M.; Madden, D.; Mašín, Z.; Plummer, M.; Tennyson, J.; Varambhia, H. UKRmol: a low-energy electron- and positron-molecule scattering suite. *Euro. Phys. J. D* **2012**, *66*, 58.
25. Semaniak, J.; Minaev, B.F.; Derkatch, A.M.; Hellberg, F.; Neau, A.; RosÃ©n, S.; Thomas, R.; Larsson, M.; Danared, H.; PaÃ¡l, A.; et al. Dissociative Recombination of HCNH+: Absolute Cross-Sections and Branching Ratios. *The Astrophysical Journal Supplement Series* **2001**, *135*, 275. https://doi.org/10.1086/321797.
26. Fortenberry, R.C.; Lee, T.J.; Inostroza-Pino, N. The possibility of :CNH2+ within Titan's atmosphere: Rovibrational analysis of :CNH2+ and :CCH2. *Icarus* **2019**, *321*, 260–265. https://doi.org/https://doi.org/10.1016/j.icarus.2018.11.026.
27. Allen, T.L.; Goddard, J.D.; Schaefer, Henry F., I. A possible role for triplet H2CN+ isomers in the formation of HCN and HNC in interstellar clouds. *The Journal of Chemical Physics* **1980**, *73*, 3255–3263, [https://pubs.aip.org/aip/jcp/article-pdf/73/7/3255/18924883/3255_1_online.pdf]. https://doi.org/10.1063/1.440520.
28. Fonseca dos Santos, S.; Douguet, N.; Kokoouline, V.; Orel, A. Scattering matrix approach to the dissociative recombination of HCO+ and N2H+. *J. Chem. Phys.* **2014**, *140*, 164308.

29. Kokoouline, V.; Ayouz, M.; Mezei, J.Z.; Hassouni, K.; Schneider, I.F. Theoretical study of dissociative recombination and vibrational excitation of the ion by an electron impact. *Plasma Sources Sci. Technol.* **2018**, *27*, 115007.
30. Yuen, C.H.; Ayouz, M.A.; Balucani, N.; Ceccarelli, C.; Schneider, I.F.; Kokoouline, V. Dissociative recombination of CH2NH2+: a crucial link with interstellar methanimine and Titan ammonia. *Monthly Notices of the Royal Astronomical Society* **2019**, *484*, 659–664, [https://academic.oup.com/mnras/article-pdf/484/1/659/27524527/sty3514.pdf]. https://doi.org/10.1093/mnras/sty3514.
31. Ayouz, M.A.; Yuen, C.H.; Balucani, N.; Ceccarelli, C.; Schneider, I.F.; Kokoouline, V. Dissociative electron recombination of NH2CHOH+ and implications for interstellar formamide abundance. *Monthly Notices of the Royal Astronomical Society* **2019**, *490*, 1325–1331, [https://academic.oup.com/mnras/article-pdf/490/1/1325/30138521/stz2658.pdf]. https://doi.org/10.1093/mnras/stz2658.
32. Mezei, J.Z.; Ayouz, M.; Orbán, A.; Abdoulanziz, A.; Talbi, D.; Kashinski, D.O.; Bron, E.; Kokoouline, V.; Schneider, I.F. Dissociative recombination of N_2H^+: a revisited study. *Eur. Phys. J. Spec. Top.* **2023**, *232*, 1967–1973.
33. Werner, H.J.; Knowles, P.J.; Knizia, G.; Manby, F.R.; Schütz, M. Molpro: a general-purpose quantum chemistry program package. *WIREs Comput. Mol. Sci.* **2012**, *2*, 242–253.
34. III, J.; D, R. NIST computational chemistry comparison and benchmark database, NIST Standard Reference Database Number 101. *NIST, Gaithersburg, MD* **2022**.
35. Conrad, M.P.; Schaefer, H.F. Role of different isomers of the H_2CN^+ ion in the formation of interstellar HCN and HNC. *Nature* **1978**, *274*, 456–457.
36. Sarpal, B.K.; Pfingst, K.; Nestmann, B.M.; Peyerimhoff, S.D. Study of electron scattering by using the polyatomic R-matrix method. *J. Phys. B: At., Mol. Opt. Phys.* **1996**, *29*, 857.
37. Maeda, S.; Harabuchi, Y.; Ono, Y.; Taketsugu, T.; Morokuma, K. Intrinsic reaction coordinate: Calculation, bifurcation, and automated search. *International Journal of Quantum Chemistry* **2015**, *115*, 258–269, [https://onlinelibrary.wiley.com/doi/pdf/10.1002/qua.24757]. https://doi.org/ https://doi.org/10.1002/qua.24757.
38. Tennyson, J.; Brown, D.B.; Munro, J.J.; Rozum, I.; Varambhia, H.N.; Vinci, N. Quantemol-N: an expert system for performing electron molecule collision calculations using the R-matrix method. *J. Phys. Conf. Series* **2007**, *86*, 012001.
39. Kokoouline, V.; Greene, C.H. Theoretical study of the H_3^+ ion dissociative recombination process. *Journal of Physics: Conference Series* **2005**, *4*, 74. https://doi.org/10.1088/1742-6596/4/1/010.
40. Ayouz, Mehdi.; Faure, Alexandre.; Kokoouline, Viatcheslav. Theoretical study of the electron-induced vibrational excitation of H2O. *AA* **2024**, *687*, A3. https://doi.org/10.1051/0004-6361/202449361.